Electronic Supplementary Material (ESI) for Environmental Science: Nano.

Supporting Information

Molecular composition determines the adsorption behaviors of loosely- and tightly-bound extracellular polymeric substances (EPS) from *Shewanella oneidensis* MR-1 on hematite nanoparticles

Mingzhao Zou[a], Yichao Wu[a,*], Chenchen Qu[a], Dengjun Wang[b], Jun Liu[a], Qiaoyun Huang[a], Peng Cai[a]

[a]State Key Laboratory of Agricultural Microbiology, College of Resources and Environment, Huazhong Agricultural University, Wuhan 430070, China.

[b]School of Fisheries, Aquaculture and Aquatic Sciences, Auburn University, Auburn, AL 36849, USA.

Corresponding author.

Email: wuyichao@mail.hzau.edu.cn (Y.W.)

Supplementary Methods:

Synthesis of Hematite. The hematite NPs were synthesized by adding 300 mL of 1 M KOH and 50 mL of 1 M $NaHCO_3$ into 500 mL of preheated 0.2 M $Fe(NO_3)_3 \cdot 9H_2O$ solution. The mixture was aged in the oven at 90 °C for 48 h. The resulting particles were separated by centrifugation at 5,000 g for 5 min and then washed by Milli-Q water until the conductivity of supernatant was below 15 S/m.

Determination of hydrophobicity. The hydrophobicity of the EPS and hematite NPs were evaluated in terms of the free energy of the interfacial interaction, ΔG. [1, 2]

$$\Delta G_{iwi} = -2\left(\sqrt{\gamma_i^{LW}} - \sqrt{\gamma_w^{LW}}\right)^2 - 4\left(\sqrt{\gamma_i^{+}} - \sqrt{\gamma_w^{+}}\right)\left(\sqrt{\gamma_i^{-}} - \sqrt{\gamma_w^{-}}\right) \quad (1)$$

where γ^{LW} is the Lifshitz–van der Waals (LW) component of the surface tension (mJ/m^2), and γ+ and γ− are the electron-acceptor and electron-donor characteristics of the Lewis acid/base component of the surface tension (mJ/m^2), respectively. When ΔG > 0, the surface is hydrophilic, otherwise it is hydrophobic. Therefore, the hydrophobicity of the surfaces decreases with an increase in ΔG.

The surface tension parameters (γ^{LW}, γ+, γ−) were determined through the contact angle measurements using three probe liquids (diiodomethane, ultrapure water and glycerol). The surface tension was determined based on Young's equation:

$$(1 + \cos\theta)\gamma_l^{Tot} = 2\left(\sqrt{\gamma_S^{LW}\gamma_l^{LW}} + \sqrt{\gamma_S^{+}\gamma_l^{-}} + \sqrt{\gamma_S^{-}\gamma_l^{+}}\right) \quad (2)$$

where θ is the contact angle of liquid l on solid s, and the γ with subscript *l* are surface tension properties of the probe liquids (Table S1). Prior to the contact angle measurements, hematite NPs and EPS were coated on glass slides by drying the aqueous NPs and EPS suspensions.[3] The contact angles were measured using a

goniometer (Drop Shape Analysis System, DSA25, Krüss GmbH, Hamburg) through the static sessile drop method.

EDLVO theory calculation. The EDLVO theory was applied to calculate the interaction energy between the hematite and EPS. This theory describes EPS interaction with hematite as a balance between LW force, Lewis acid/base interaction (AB) and electrostatic force (EL):[3]

$$G^{Tot}(d) = G^{LW}(d) + G^{AB}(d) + G^{EL}(d) \quad (3)$$

where $G^{Tot}(d)$ is the interaction energy between EPS and hematite at a certain distance (d), and different superscripts stand for different types of forces. The model for sphere–plate was selected to evaluate the interaction energy between EPS and hematite. The van der Waals attractive interaction energy was calculated using the following equation:[4]

$$G^{LW}(d) = -\frac{A_{1W2}a}{12d}\left[1 + \frac{14d}{\lambda}\right]^{-1} \quad (4)$$

where d is separation distance; a is radius of EPS; λ is the characteristic wavelength (usually taken as 100 nm); A_{1W2} is the Hamaker constant for EPS and hematite in water was calculated by using the following equation:[5]

$$A_{1W2} = 24\pi d_0^2\left(\sqrt{\gamma_1^{LW}} - \sqrt{\gamma_w^{LW}}\right)\left(\sqrt{\gamma_2^{LW}} - \sqrt{\gamma_w^{LW}}\right) \quad (5)$$

The electrostatic double layer interaction can be determined according to the following equation:

$$G^{EL}(d) = \pi\varepsilon a\left[2\varphi_1\varphi_2 \ln\left(\frac{1 + e^{-kd}}{1 - e^{-kd}}\right) + (\varphi_1^2 + \varphi_2^2)\ln\left(1 - e^{-2kd}\right)\right] \quad (6)$$

where ε is the permittivity of water (6.96×10^{-10} $m^{-1}V^{-2}$); φ is zeta potential; κ is

the double-layer thickness^{-1} ($0.328\times10^{10}\times I^{0.5}$/m).

$$G^{AB}(d) = 2\pi a\lambda_{AB}G_{d0}^{AB}exp\left[\frac{d_0 - d}{\lambda_{AB}}\right] \quad (7)$$

where λ_{AB} is the decay length of water, taken as 0.5 nm; The distance of closest approach, d_0, is taken as 0.157 nm. G_{d0}^{AB} is the Lewis acid/base free energy (J/m^2) for the EPS-mineral interaction at a minimum separation distance (d_0) and can be determined from the surface tension parameters:

$$\Delta G_{d0}^{AB} = 2\left(\sqrt{\gamma_1^+} - \sqrt{\gamma_2^+}\right)\left(\sqrt{\gamma_1^-} - \sqrt{\gamma_2^-}\right) - 2\left(\sqrt{\gamma_1^+} - \sqrt{\gamma_w^+}\right)\left(\sqrt{\gamma_1^-} - \sqrt{\gamma_w^-}\right) - 2\left(\sqrt{\gamma_2^+} - \sqrt{\gamma_w^+}\right)\left(\sqrt{\gamma_2^-} - \sqrt{\gamma_w^-}\right) \quad (8)$$

QCM-D Measurements. The hematite NPs (0.01 g) were suspended in 10 mL methanol, and stirred overnight. Forty μL of suspension was dropped onto a spin coater at a speed 6,000 rpm and an acceleration of 100 rpm/s for 60 s. Specific QCM-D sensors were mounted in the flow modules and placed into the measuring chamber. Prior to the introduction of EPS solutions, the quartz crystal sensor was equilibrated with 0.1 M NaCl background solution to obtain a stable frequency and dissipation baseline.

The elastic shear modulus and thickness of the adsorbed EPS layers were determined with the Voigt-based viscoelastic model [6]. The thickness (h_q) and density (ρ_q) of quartz crystals were 3×10^{-4} m and 2650 kg·m^{-3}, respectively. The adsorbed EPS layer was represented by thickness (h_f), density (ρ_f), shear viscosity (η_f), and elastic shear modulus (μ_f). The shift in frequency (Δf) and dissipation (ΔD) were calculated as follows:

$$\Delta f = Im\left(\frac{\beta}{2\pi\rho_q h_q}\right) \tag{9}$$

$$\Delta D = -Re\left(\frac{\beta}{\pi\rho_q h_q}\right) \tag{10}$$

β was determined as follows:

$$\beta = \xi_1\left(\frac{2\pi f\eta_f - i\mu_f}{2\pi f}\right)\left[\frac{1-\alpha\, exp(2\xi_1 h_f)}{1+\alpha\, exp(2\xi_1 h_f)}\right] \tag{}$$

$$\alpha = \frac{\left(\frac{\xi_1}{\xi_2}\right)\left(\frac{2\pi f\eta_f - i\mu_f}{2\pi f n_l}\right)+1}{\left(\frac{\xi_1}{\xi_2}\right)\left(\frac{2\pi f\eta_f - i\mu_f}{2\pi f n_l}\right)-1}$$

$$\xi_1 = \sqrt{-\frac{(2\pi f)^2\rho_f}{\mu_f + i2\pi f\eta_f}}$$

$$\xi_2 = \sqrt{i\left(\frac{2\pi f\rho_l}{\eta_l}\right)}$$

where the subscripts q, f, and l refer to the crystal, film, and bulk liquid, respectively. The measured Δf and ΔD at different overtones were fitted to the model to estimate the elastic shear modulus and thickness of the adsorbed EPS layers.

ATR-FTIR Measurements. ATR-FTIR measurements were performed using a spectrometer (IFS66 v/s, Bruker, Karlsruhe, Germany) equipped with a Mercury Cadmium Telluride (MCT)-(MIR) liquid nitrogen-cooled detector and OPUS 5.5 processing software.[7] All spectra were collected at pH 7.0, with 256 scans over the 1800–800 cm^{-1} range at a resolution of 4 cm^{-1} every 5 mins to monitor the adsorption process over time. A horizontal attenuated total reflectance flow cell with a 45° ZnSe ATR crystal was used and 10 internal reflections were yielded at the sample surface. One mL of 1 mg/mL hematite NPs suspension was evenly spread across the crystal

surface and dried for 12 h at 37 °C.[8] The coated crystal was sealed in a flow cell and placed on the ATR stage inside the IR spectrometer. The EPS samples (20 mg/L TOC) were subsequently introduced at the same flow rate for 7 h.

2D-FTIR-COS Analysis. After smoothing and baseline correction for the IR spectra using Omnic 8.0 software, 2D-COS analysis was performed using 2Dshige software (Shigeaki Morita, Japan). In this analysis, the contact time was used as the external perturbation for the complexation of EPS with hematite. The calculations were carried out by using Origin 9.0. An analytical spectrum $U(v, t)$ is considered to illustrate how the technique works. The variable v is the index variable for the FTIR spectra caused by the perturbation variable t. A discrete set of dynamic spectra measured at m equally spaced points in time t between T_{min} and T_{max} can be expressed as follows:

$$U_j(v) = y(v,t_j), j = 1, 2, \ldots, m \quad (15)$$

A set of dynamic spectra can be represented by the following equation:

$$\tilde{U}(v, t) = U(v, t_j) - \bar{U}(v) \quad (16)$$

where $\bar{U}(v)$ represents the reference spectrum, which is generally the average spectrum and can be expressed as follows:

$$\bar{U}(v) = \frac{1}{m}\sum_{j=1}^{m} U(v,t_j) \quad (17)$$

The synchronous correlation intensity can be directly obtained from the following equation:

$$\Phi(v_1,v_2) = \frac{1}{m-1}\sum_{j=1}^{n} \tilde{U}_j(v_1)\tilde{U}_j(v_2) \quad (18)$$

The asynchronous correlation intensity can be obtained as follows:

$$\Psi(v_1,v_2) = \frac{1}{m-1}\sum_{j=1}^{m}\tilde{U}_j(v_1)\sum_{k=1}^{m}M_{jk}\tilde{U}_j(v_2) \quad (19)$$

The term M_{jk} corresponds to the j^{th} column and the k^{th} raw element of the discrete Hibert-Noda transformation matrix, which can be expressed by the following equation:

$$M_{jk} = \begin{cases} 0 & if\ j = k \\ \dfrac{1}{\pi(k-j)} & otherwise \end{cases} \quad (20)$$

The intensity of a synchronous correlation spectrum $\Phi(v_1,v_2)$represents the simultaneous or coincidental changes of two separate spectral intensity variations measured at v_1 and v_2 during the interval between T_{min} and T_{max} of the externally defined variable *t*. The intensity of an asynchronous spectrum $\Phi(v_1,v_2)$ represents sequential or successive, but not coincidental, changes of spectral intensities measured separately at v_1 and v_2. The rank order of intensity change between two bands at v_1 and v_2 can be obtained from the signs of the synchronous correlation peak $\Phi(v_1,v_2)$ and asynchronous correlation peak $\Psi(v_1,v_2)$ based on previously established principles.[9-11] Briefly, for asynchronous cross peak, the sign becomes positive if the spectral intensities at the two bands at v_1 and v_2 corresponding to the coordinates of the cross peak are either increasing or decreasing together as functions of the external variable *t* during the observation interval, otherwise, the sign becomes negative; while for an asynchronous cross peak, the sign becomes positive if the intensity change at v_1 occurs predominantly before that at v_2 in the sequential order of *t*, otherwise, the sign becomes negative. If $\Phi(v_1,v_2)$ and $\Psi(v_1,v_2)$ have the same signs, the changes in the spectral intensity at band v_1 will occur prior to those at v_2; if they have opposite signs, the order will be reversed. If $\Psi(v_1,v_2)$ is zero, then the changes at v_1 and v_2 will

occur simultaneously.[8-10]

As the changes in spectral intensity represent the interaction of the corresponding IR bands and EPS functional groups, then the order in which the spectral intensity changes appear reflects the order in which the IR bands and thus the corresponding EPS functional groups interact with the hematite surface. In this way, the results obtained from the 2D-COS can reflect the order in which the different EPS functional groups interact and bind with hematite.

Supplementary Figures and Tables.

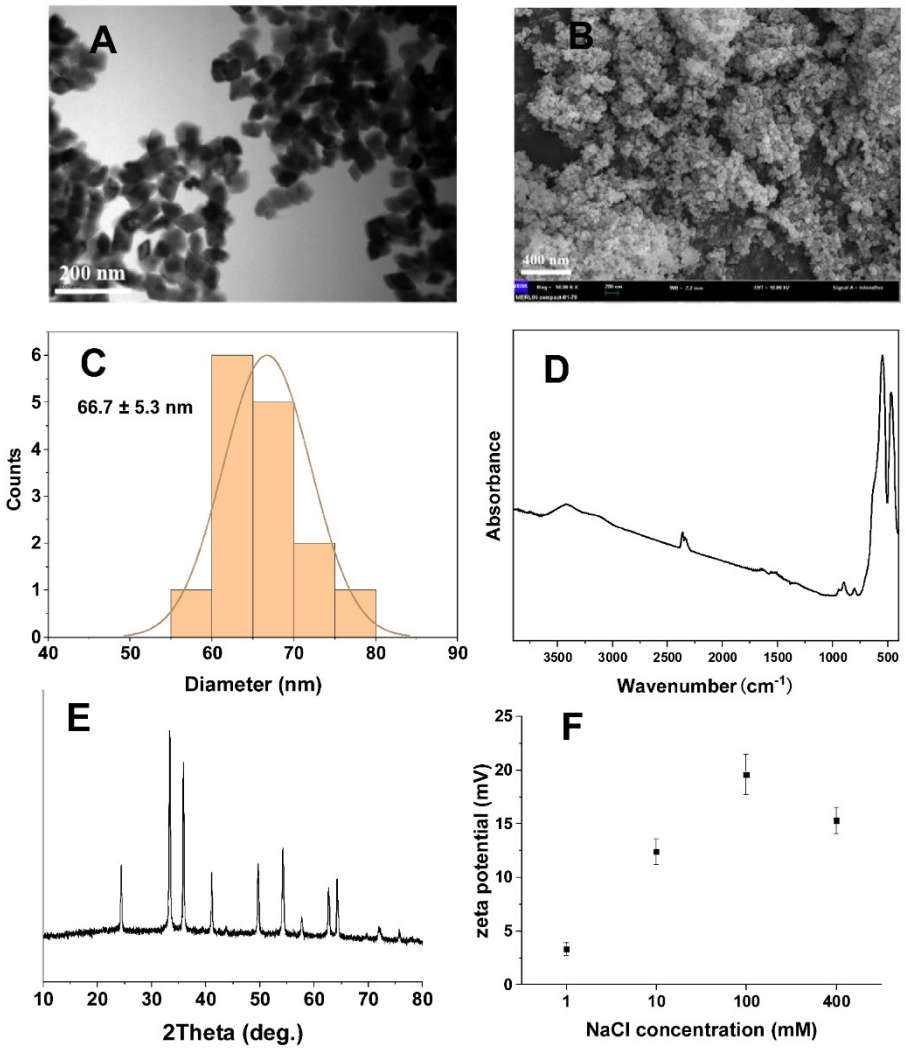

Figure S1. The TEM images (A), SEM images (B), diameter distribution (C), FTIR spectrum (D), XRD pattern (E), and the zeta potential (F) of hematite NPs. Zeta potential measurements were carried out in different concentrations of NaCl solution at pH 7.0.

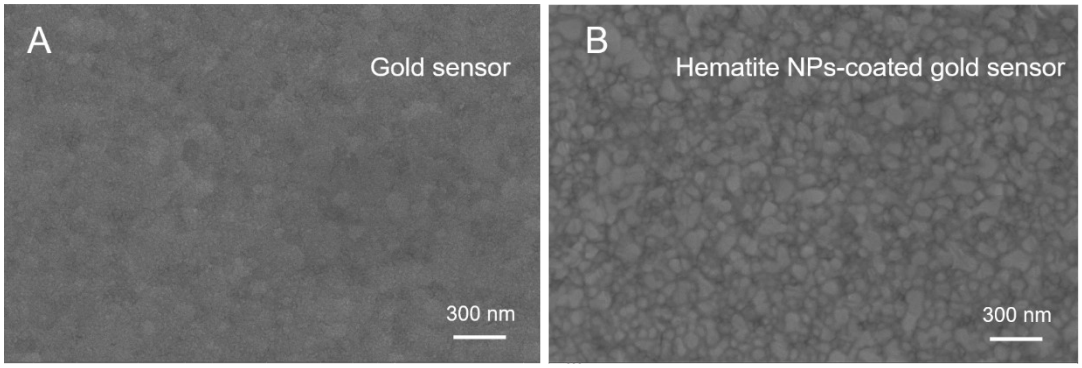

Figure S2. SEM images of the gold sensor (A) and hematite NPs-coated gold sensor (B).

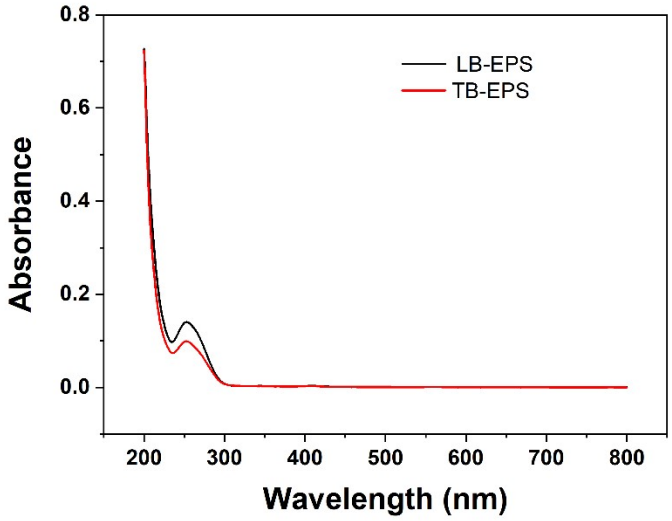

Figure S3. UV–vis absorption spectra of LB-EPS and TB-EPS.

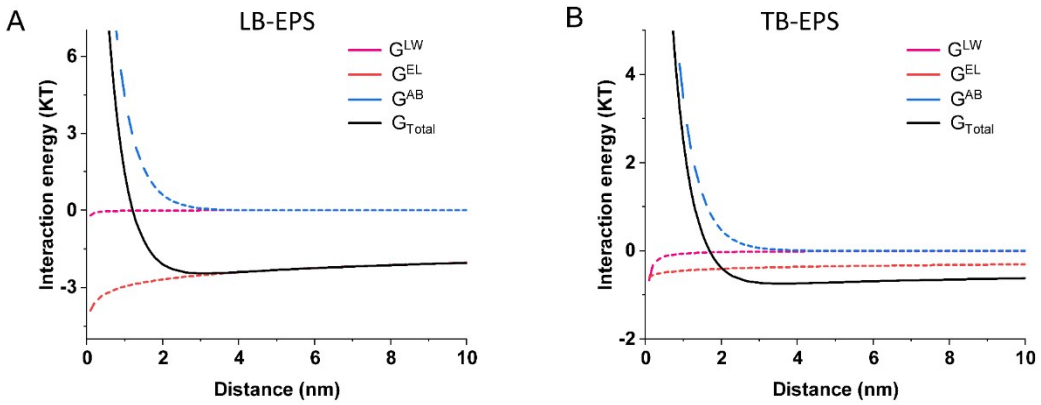

Figure S4. Profiles for the EDLVO simulations of the Lifshitz–van der Waals (LW) force, Lewis acid/base interaction (AB) and electrostatic force (EL), and total interaction energy between LB-EPS (A) and TB-EPS (B) with hematite NPs.

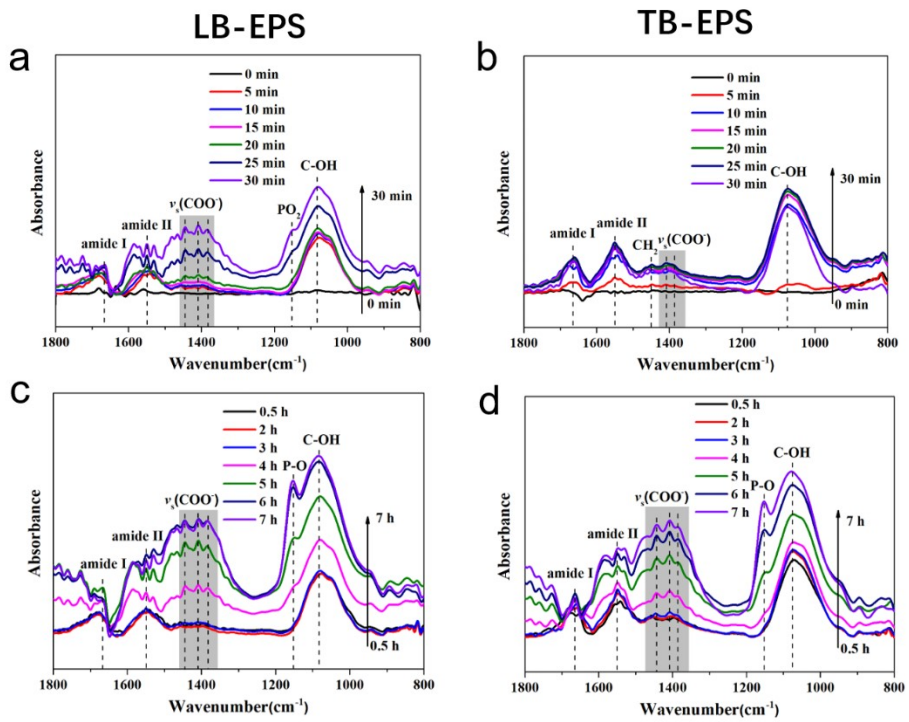

Figure S5. ATR-FTIR spectra (0-0.5 and 0.5-7 h) as a function of time during the LB-EPS and TB-EPS adsorption processes on hematite surface, respectively.

Table S1. Surface tension parameters of probe liquids used for contact angle measurements.[12]

	Surface tension parameters (mJ m^{-2})			
	γ^{LW}	$\gamma+$	$\gamma-$	γ^{Tot}
H_2O	21.8	25.5	25.5	72.8
CH_3NO	39.0	2.3	39.6	58.0
CH_2I_2	50.8	0	0	50.8

Table S2. EEM Fluorescence spectra parameters of original LB-EPS and TB-EPS samples.

EPS	Peak A		Peak B		Peak C		Peak D	
	Ex/Em (nm) (AU)	Intensity	Ex/Em (nm) (AU)	Intensity	Ex/Em (nm) (AU)	Intensity	Ex/Em (nm)	Intensity (AU)
LB-EPS	225/310	1756.3	275/315	1115.8	440/355	23.3	-	
TB-EPS	225/325	1532.4	275/330	965.7	420/355	27.5	355/530	15.1

Table S3. Liquid-solid contact angles and hydrophobicity of EPS and hematite NPs

	Contact angles (degree)			Surface tension parameters (mJ m^{-2})			ΔG (mJ m^{-2})
	H_2O	CH_3NO	CH_2I_2	γ^{LW}	γ+	γ-	
Hematite	17.5±0.7	11.0±1.7	13.2±1.4	49.3	0.2	56.7	34.6
LB-EPS	18.1±1.2	26.7±3.2	68.1±4.8	23.8	0.6	84.6	70.8
TB-EPS	31.7±3.6	23.8±1.9	58.9±3.2	28.9	3.61	42.9	17.9

Table S4. FTIR vibrational frequencies and assignments for EPS [8, 13, 14].

Wavenumber (cm^{-1})	functional group assignment
1656-1668	stretching C=O in amides (Amide I band) bending -NH and $-NH_2$ of amine
1546-1552	N-H bending and C-N stretching in amides (Amide II band); bending -NH and $-NH_2$ of amines
1454-1482	bending of CH_2/CH_3
1395-1411	υ_s (COO^-)
1150-1160	V(P-O) of phosphoryl surface complexes
1084-1094	$\nu_s(PO_2^-)$ of monodentate surface complexes
1068-1078	C-OH, C-O-C, and C-C vibrations of polysaccharides

Table S5. Signs of each cross-peak in the synchronous and asynchronous correlation contour maps of LB-EPS adsorption on hematite for 0-0.5 h.

Wavenumber (cm^{-1})	1662	1546	1407	1150	1078
1662	+	+(-)	+(-)	+(-)	+(+)
1546		+	+(-)	+(-)	+(+)
1407			+	+(-)	+(+)
1150					+(+)
1078					+

Table S6. Signs of each cross-peak in the synchronous and asynchronous correlation contour maps of LB-EPS adsorption on hematite for 0.5-7 h.

Wavenumber (cm^{-1})	1664	1548	1407	1150	1078
1664	+	+(-)	+(+)	+(+)	+(+)
1548		+	+(+)	+(+)	+(+)
1407			+	+(-)	+(+)
1150					+(+)
1078					+

Table S7. Signs of each cross-peak in the synchronous and asynchronous correlation contour maps of TB-EPS adsorption on hematite for 0-0.5 h.

Wavenumber (cm^{-1})	1656	1546	1454	1395	1068
1656	+	+(-)	+(-)	+(-)	+(-)
1546		+	+(-)	+(-)	+(-)
1454			+	+(-)	+(-)
1395					+(+)
1068					+

Table S8. Signs of each cross-peak in the synchronous and asynchronous correlation contour maps of TB-EPS adsorption on hematite for 0.5-7 h.

Wavenumber (cm^{-1})	1668	1552	1411	1154	1076
1668	+	+(-)	+(+)	+(+)	+(+)
1552		+	+(+)	+(+)	+(+)
1411			+	+(+)	+(+)
1154					+(+)
1076					+

Table S9. EEM Fluorescence spectra parameters of unadsorbed LB-EPS and TB-EPS in the effluent from FTIR flow cells.

EPS	Peak A		Peak B	
	Ex/Em (nm)	Intensity (AU)	Ex/Em(nm)	Intensity (AU)
LB-EPS	225/310	126.3	275/315	46.8
TB-EPS	225/310	556.3	275/305	315.4

Supplementary References:

1 C. Oss, Hydrophobicity of biosurfaces — Origin, quantitative determination and interaction energies, *Colloid. Surface. B.*, 1995, **5**, 91-110.

2 C. Qu, S. Qian, L. Chen, Y. Guan, L. Zheng, S. Liu, W. Chen, P. Cai and Q. Huang, Size-Dependent Bacterial Toxicity of Hematite Particles, *Environ. Sci. Technol.* 2019, **53**, 8147-8156.

3 Z. N. Hong, X. M. Rong, P. Cai, K. Dai and Q. Huang, Initial adhesion of *Bacillus subtilis* on soil minerals as related to their surface properties, *Eur. J. Soil Sci.*, 2012, **63**, 457-466.

4 C. Peng, Q. Huang and S. L. Walker, Deposition and Survival of *Escherichia coli* O157:H7 on Clay Minerals in a Parallel Plate Flow System, *Environ. Sci. Technol.*, 2013, **47**, 1896-1903.

5 P. K. Sharma and K. H. Rao, Adhesion of *Paenibacillus polymyxa* on chalcopyrite and pyrite: surface thermodynamics and extended DLVO theory, *Colloid. Surface. B.*, 2003, **29**, 21-38.

6 Z. Liu, H. Choi, P. Gatenholm and A. R. Esker, Quartz crystal microbalance with dissipation monitoring and surface plasmon resonance studies of carboxymethyl cellulose adsorption onto regenerated cellulose surfaces, *Langmuir*, 2011, 27, 8718-8728.

7 W. Yan, J. Zhang and C. Jing, Adsorption of Enrofloxacin on montmorillonite: Two-dimensional correlation ATR/FTIR spectroscopy study, *J. Colloid Interf. Sci.*, 2013, **390**, 196-203.

8 P. Cai, D. Lin, C. L. Peacock, W. Peng and Q. Huang, EPS adsorption to goethite: Molecular level adsorption mechanisms using 2D correlation spectroscopy, *Chem. Geol.*, 2018, **494**, 127-135.

9 A. Domínguez-Vidal, M. P. Saenz-Navajas, M. J. Ayora-Cañada and B. Lendl, Detection of albumin unfolding preceding proteolysis using Fourier transform infrared spectroscopy and chemometric data analysis, *Anal. Chem.*, 2006, **78**, 3257-3264.

10 Q. Jia, N.-N. Wang and Z.-W. Yu, An insight into sequential order in two-dimensional correlation spectroscopy, *Appl. Spectrosc.*, 2009, **63**, 344-353.

11 I. Noda and Y. Ozaki, Two-dimensional correlation spectroscopy: applications in vibrational and optical spectroscopy, John Wiley & Sons, 2005.

12 R. Oliveira, J. Azeredo, P. Teixeira and A. Fonseca, The role of hydrophobicity in bacterial adhesion, 2001.

13 W. Yan, H. Wang and C. Jing, Adhesion of *Shewanella oneidensis* MR-1 to Goethite: A Two-Dimensional Correlation Spectroscopic Study, *Environ. Sci. Technol.*, 2016, **50**, 4343-4349.

14 E. J. Elzinga, J.-H. Huang, J. Chorover and R. Kretzschmar, ATR-FTIR spectroscopy study of the influence of pH and contact time on the adhesion of *Shewanella putrefaciens* bacterial cells to the surface of hematite, *Environ. Sci. Technol.*, 2012, **46**, 12848-12855.